

Single-particle characterization of the High Arctic summertime aerosol

B. Sierau¹, R. Y.-W. Chang^{2,*}, C. Leck³, J. Paatero⁴, and U. Lohmann¹

¹Institute for Atmospheric and Climate Science, ETH Zurich, Zurich, Switzerland

²Department of Chemistry, University of Toronto, Toronto, Canada

³Department of Meteorology, Stockholm University, Stockholm, Sweden

⁴Finnish Meteorological Institute, Helsinki, Finland

* now at: Department of Earth and Planetary Sciences, Harvard University, Cambridge, USA

1. Mass spectra from individual particles

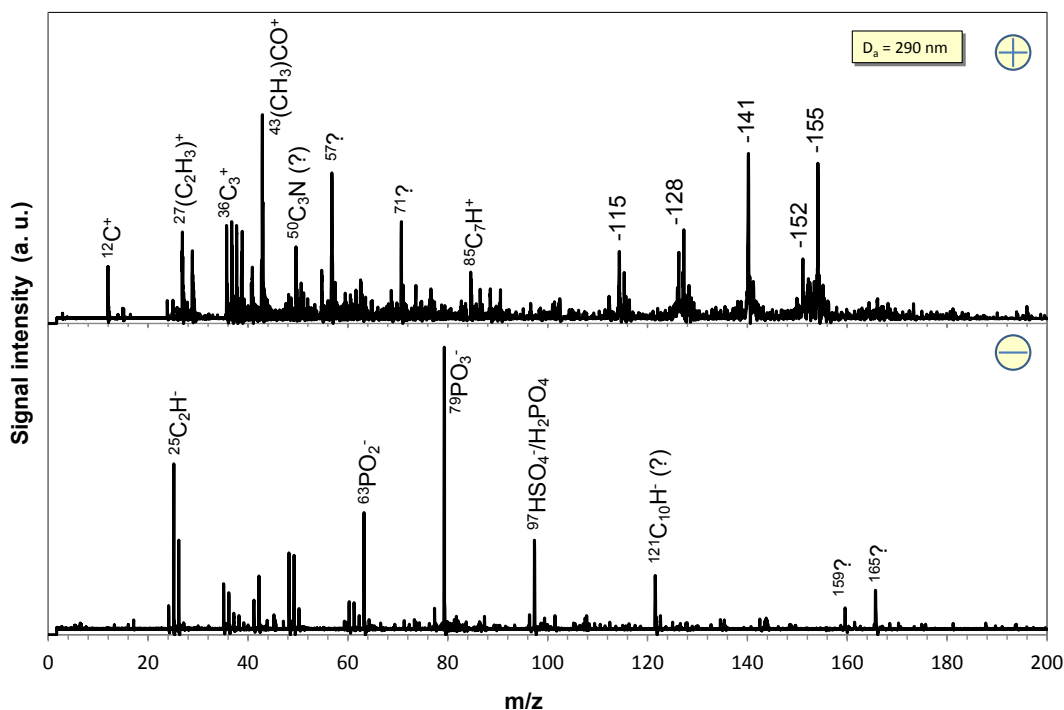


Fig. S1: Mass spectrum of an *ECOC-PAH* type particle. The upper panel depicts detected positive ions, the lower one negative ions.

Figure S1 exemplarily depicts a mass spectrum of an *ECOC-PAH* cluster type 1c particle. The mass spectrometric feature to focus on is the positive ion peak series (upper panel) at m/z 115, 128, 141, 152 that is usually attributed to PAH compounds (Gross et al., 2000; Silva and Prather, 2000). The PAH series is separated by $\Delta 13$ amu (McLafferty and Turecek, 1993).

This type of mass spectra resembles the ones measured when exhaust from the ship was sampled, and spectra are thus assigned to ship pollution particles not

sorted out by the pollution screening procedure. Also, the *ECOH-PAH* cluster type particles occurred during a strongly confined time window between 14:45 – 14:48 UTC on 26 August, supporting this assignment.

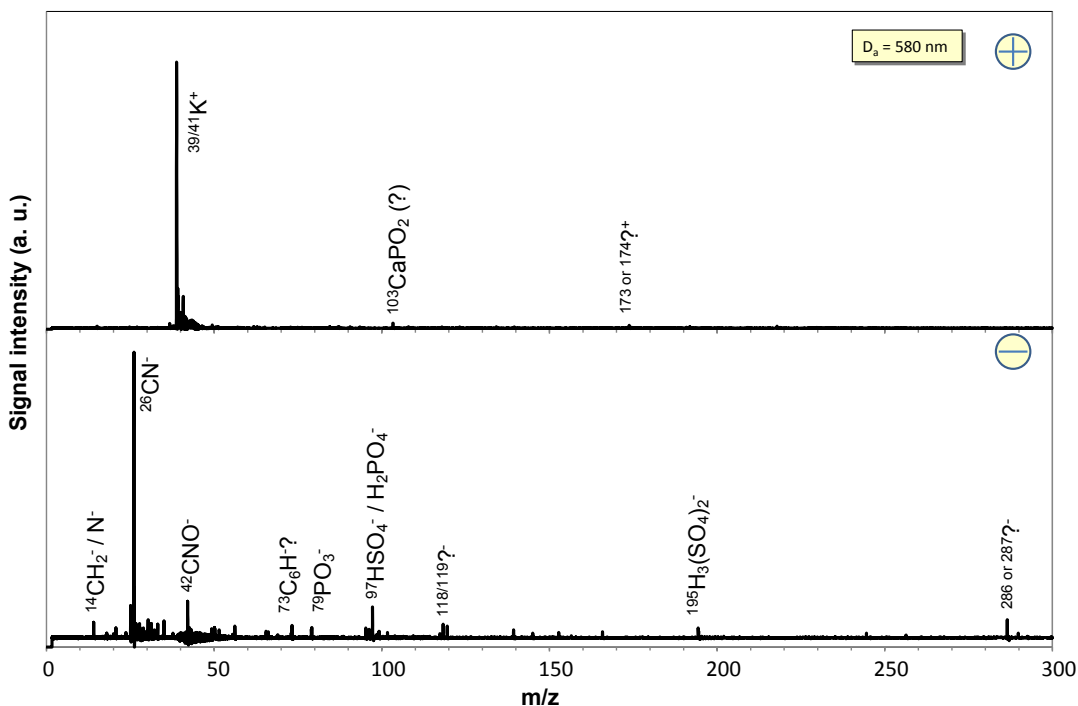


Fig. S2: Mass spectrum of a *K-CN-sulfate* type particle (cluster 3).

Figure S2 exemplarily depicts a mass spectrum of a *K-CN-sulfate* cluster type 3 particle. The mass spectrometric features to focus on are the negative ion peaks at $^{26}CN^-$, $^{42}CNO^-$, and $^{79}PO_3^-$ which are – in combination with K, Mg, and Ca – often used as tracers for biological material (see Sec. 3.3). This individual particle spectrum shows more detail than the ENCHILADA-obtained cluster spectrum presented in the main paper (Fig. 8), and, among others, reveals minor peaks that couldn't be assigned to certain ions (e.g. m/z +173 or +174, m/z -118/-119). However, based on the identified minor ion peaks, additional evidence for an assignment of this particle to an ocean-derived particle type as discussed in Sec. 3.3 of the manuscript cannot be adduced. Further investigations on this type of particle are presented and discussed below in the supplementary section 3.

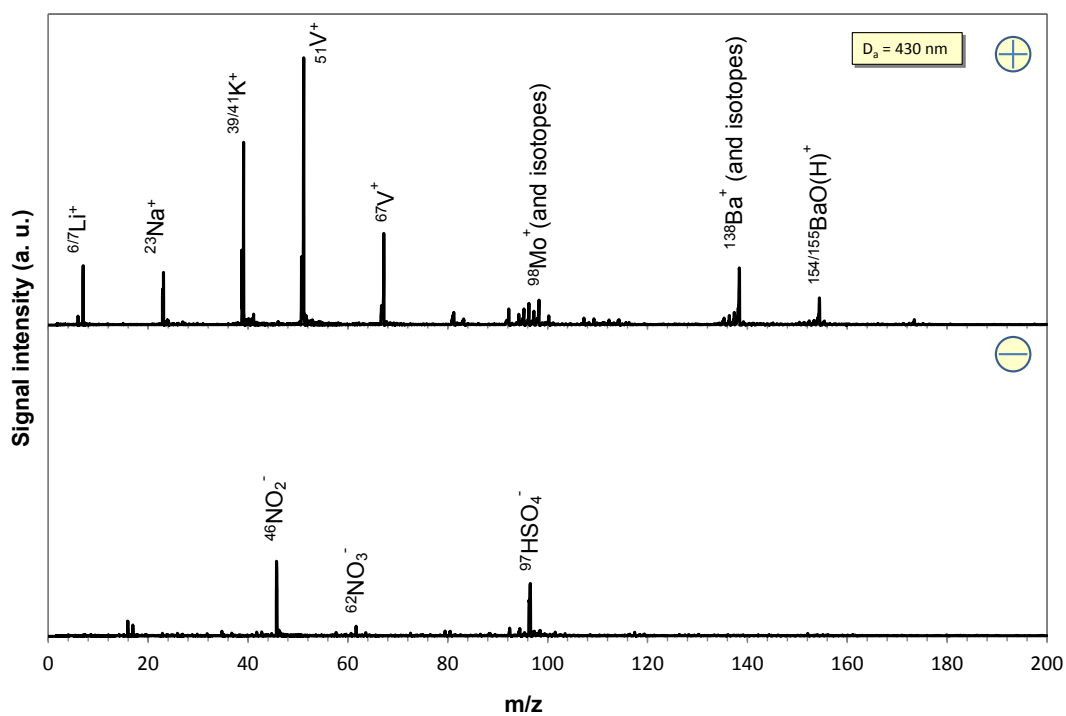


Fig. S3: Mass spectrum of a *metal* type particle (cluster 4).

Figure S3 exemplarily depicts a mass spectrum of a *metal* type 4 particle. The mass spectrometric features to focus on are the peaks occurring in the positive spectrum that were assigned to the metal components Li, V, Mo, and Ba. In addition to those, traces of Fe, Al and Ag have been detected in individual particles as well.

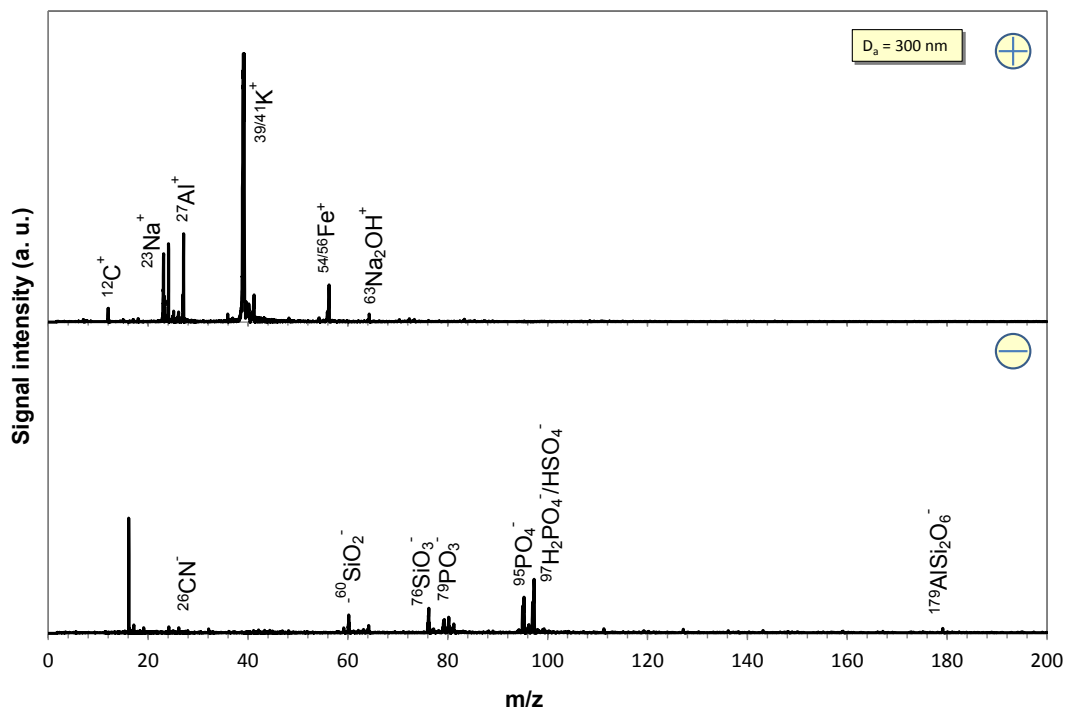


Fig. S4: Mass spectrum of a *soil dust* type particle (cluster 5).

Figure S4 exemplarily depicts a mass spectrum of a *soil dust* type 5 particle. The spectrum contains ions peaks assigned to K, Al, Fe and Si which are markers for dust. Also, Ca-dominated particles have been observed. The occurrence of peaks at m/z -26, -79, and -95 points to the ions $^{26}\text{CN}^-$, $^{79}\text{PO}_3^-$, and $^{95}\text{PO}_4^-$, respectively, which are potential markers for biological material, thus the assignment of this type to *soil dust*. Note that the assignment of m/z +27 ($^{27}\text{Al}^+$), m/z -60 ($^{60}\text{SiO}_2^-$) and m/z -76 ($^{76}\text{SiO}_3^-$) interferes with $^{27}\text{C}_2\text{H}_3^+$, $^{60}\text{AlO}(\text{OH})^-$, $^{76}\text{AlO}_2(\text{OH})^-$, respectively.

2. Mass spectra of individual cluster types

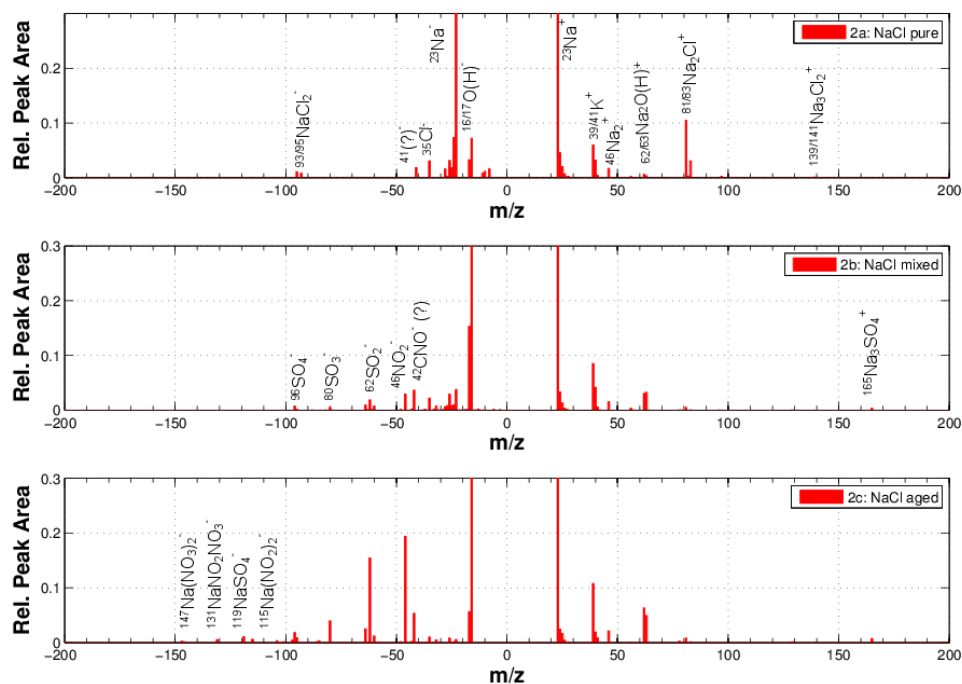


Fig. S5: Cluster spectra of sea salt types *NaCl pure*, *mixed* and *aged* (cluster 2a, 2b, 2c, respectively).

Figure S5 depicts the mass spectra of the *NaCl* cluster centers (type 2a “*NaCl pure*”, 2b “*NaCl mixed*”, 2c “*NaCl aged*”) as obtained for the IF station. From the “pure” to “aged” particle composition, nitrate and sulfate compound ions appear whereas chloride ions disappear. This reflects the compositional change of *NaCl* aerosols due to atmospheric aging (Sec. 3.1.1).

3. Time traces of individual cluster types

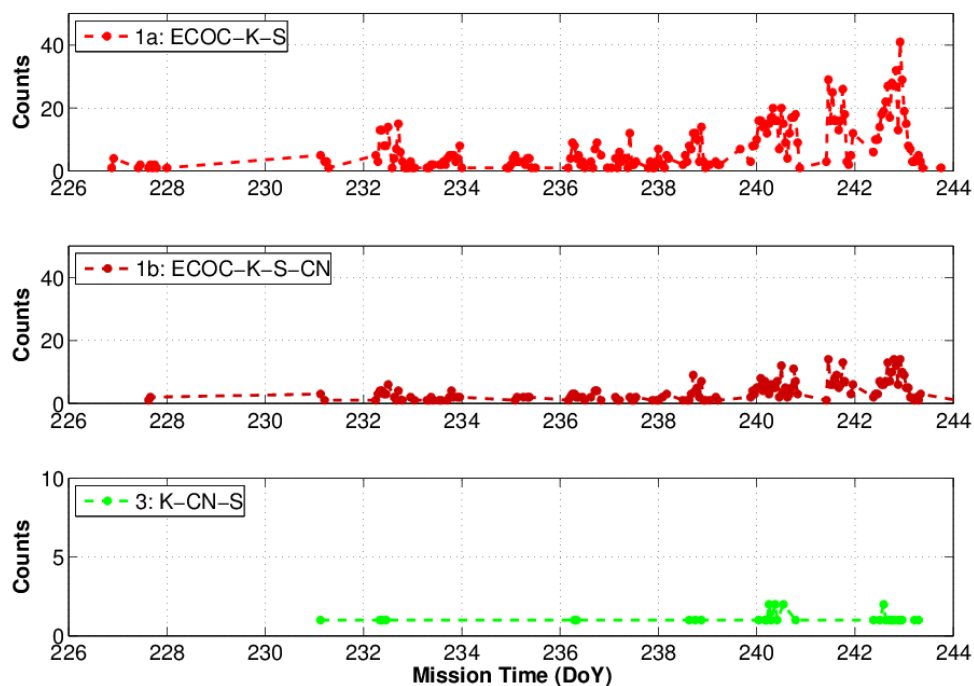


Fig. S6: Time line of 1h-summed *ECOC* types 1a, 1b (upper and middle panel) and *K-CN-S* type (lower panel) particles detected at the IF station.

Figure S6 depicts the time traces of the *ECOC-K-sulfate* (type 1a), *ECOC-K-sulfate-CN* (type 1b), and the *K-CN-S* (type3) cluster particles as present during the IF station. The latter one is discussed in Sec. 3.3 as potentially presenting an ocean-derived aerosol of biogenic origin. The time trace of cluster type 1d particles was not plotted, as those were not present during this time period.

The temporal correlation between type 1a and type 1b strongly supports the relation of both cluster types - expressed in their common affiliation to the inorganic carbonaceous family 1. Based on the temporal correlation and the mass spectrometric similarities, an assignment to a similar particle type is suggested.

The time trace of the *K-CN-S* cluster type (lowest panel) clearly demonstrates the analysis problems arising from the lack of statistics due to the low number of sampled and detected particles (only 34 in this case). A correlated occurrence of cluster type 3 and cluster type 1a, b particles could be suspected but without statistical significance. Based on this “suggested” temporal correlation between type 1 and type 3 cluster particles, a similar source or external mixing of both particle types when reaching the ship is suggested. Mass spectrometric similarities/dissimilarities between these cluster types are discussed in the manuscript.

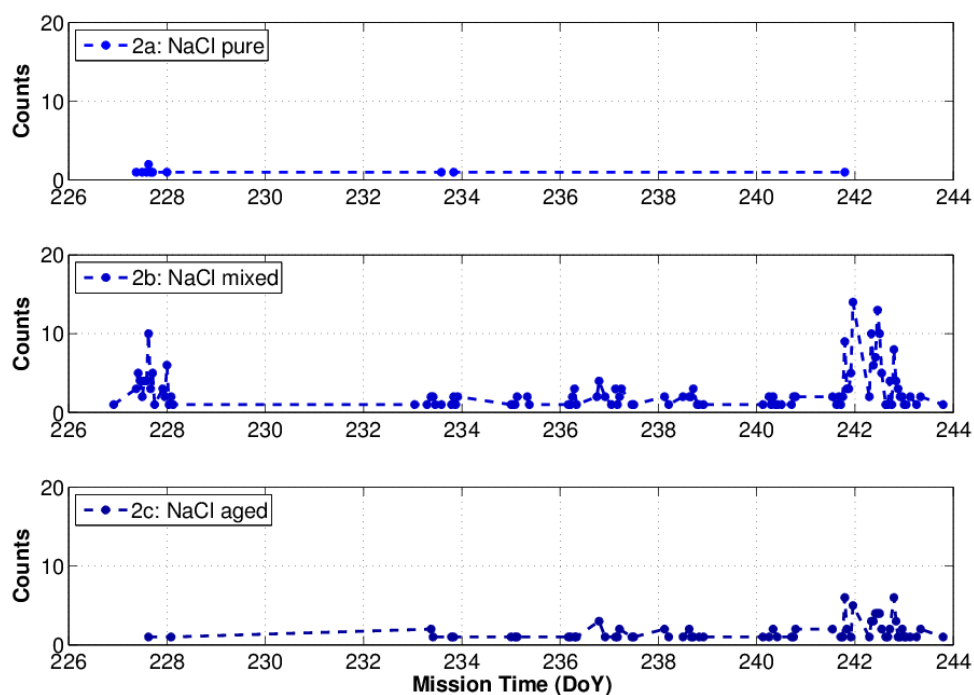


Fig. S7: Time line of 1h-summed sea salt types *NaCl pure*, *mixed*, and *aged* (cluster 2a, b, and c, respectively) particle counts at the IF station.

Figure S7 depicts the time traces of the *NaCl* cluster particles as present during the IF station. The number of counts for *NaCl mixed* and *aged* particles correlate for most of time during IF-measurement period except for the first couple of days (DoY 227 and 228). For the correlating periods, this suggests a similar transport pathway and/or source over the ice of both particle fractions before reaching the ship. The “advanced aging” of type 2c particles might then be due to a longer atmospheric residence time of those compared to type 2b particles.

Based on the comparison between the time traces of the pure, i.e. fresh *NaCl* particles (type 2a) and the potentially ocean-derived *K-CN-S* cluster type particles (type 3), a primary, sea salt connected local source of the latter type is rather unlikely.

References

Gross, D. S., Galli, M. E., Silva, P. J., Wood, S. H., Liu, D.-Y., and Prather, K. A.: Single particle characterization of automobile and diesel truck emissions in the Caldecott Tunnel, *Aerosol Sci. Tech.*, 32, 152–163, doi:10.1080/027868200303858, 2000. 607

McLafferty, F. W. and Turecek, F.: *Interpretation of Mass Spectra*, 4 edn., University Science Books, Sausalito, CA, USA, 1993. 607

Silva, P. J. and Prather, K. A.: Interpretation of mass spectra from organic compounds in aerosol time-of-flight mass spectrometry, *Anal. Chem.*, 72, 3553–3562, doi:10.1021/ac9910132, 2000. 607